



# The Effects of Radio Frequency Exposure to Edible Unwired Manifest on the Specific Absorption Rate Due to the Dielectric Values of the Human Body.

<sup>1</sup>Prof.Shivanand Konade, <sup>2</sup>Prof.Vinay Nimbalkar

<sup>1</sup> Assistant Professor, Electrical Engineering Department, Smt. Indira Gandhi College of Engineering, <sup>2</sup> Assistant Professor, Electrical Engineering Department MGM's College of Engineering and Technology

## Abstract

The finite-difference time-domain method is used to study the SAR and near fields of edible wireless devices (IWD) in two realistic human body models whose dielectric values are enhanced from the original by  $\pm 10\%$  and  $\pm 20\%$  in order to determine the compliance of IWD within safety criteria. A comparison is made between the IWD's radiation properties in the human body model with and without altered dielectric values. Thirteen scenarios are simulated, with the IWD positioned in the centre of the two models' abdomens at operating frequencies of 430, 800, and 1200 MHz, respectively. The radiation intensity variation at the abdominal surface is found to be around 2.5, 2.6, and 3.5 dB within a 20% range of the dielectric values, which correspond to frequencies of 430, 800, and 1200 MHz, respectively. Correspond to 430, 800, and 1200 MHz in frequency, in that order. In every situation, the electric fields in the anterior of the human body models are greater than those in the posterior. SAR values typically rise in proportion to the conductivities of human body tissues and fall in proportion to the relative permittivities of those tissues. The human body's dielectric properties have an orientation-, human-body-and frequency-dependent impact on SAR. At frequencies of 430, 800, and 1200 MHz, respectively, variations in conductivities and relative permittivity's up to 20% either separately or concurrently always result in SAR variations of less than 10%, 20%, and 30%. Regarding safety compliance, the IWD was deemed safe for usage at input power levels below 12.6; 9.3; and 8.4.

**Keywords-** Dielectric value, radiation properties, ingestible wireless device (IWD), finite-difference time domain (FDTD), and SAR.

## I. INTRODUCTION

Overall concerns regarding the safety of wireless devices in accordance with international safety standards have been raised by the use of wireless communication [1]–[3]. Nevertheless, the majority of them mainly examined the safety and radiation characteristics of external sources, such as wearable medical sensor equipment, even though an increasing number of implanted or ingestible devices—such as pacemakers, implanted therapeutic devices, capsule endoscopes, and implantable defibrillators—are used in clinical settings [4], [5]. The durability and high local-energy deposition of antennas embedded in human tissues have prompted recent proposals for research on the safety of ingestible or implantable wireless devices in the human body [6]. Wireless capsule endoscope [5], which enabled the transmission of high-resolution video, and wireless multiparameter monitoring of the gastrointestinal (GI) tract [7, 8] were also used. Chirwa et al. investigated the near fields and radiation patterns of ingestible wireless devices (IWD) in people. Xu et al. examined the IWD in unrealistic human body model's biological effects and radiation efficiency in 21 scenarios at frequencies between 430 MHz and 2.4 GHz. Outcomes demonstrated that elevated SAR and temperature rise values were concentrated in the vicinity of the IWD [10]. Nevertheless, it has not yet been examined how individual differences in human tissue dielectric properties affect radiation characteristics uncertainty. It is unknown how the dielectric properties of human body tissues affect the radiation characteristic of IWD. The parameters that determine the best RF communication and dosimeter are conductivity ( $\sigma$ ) and relative permittivity ( $\epsilon$ ) of human tissues. Lately, the fluctuations in dielectric parameters have been discovered in human tissues [11], [12]. The standard deviations of dielectric values for 12 samples of rat brain tissue varied from  $\pm 4\%$  to  $\pm 16\%$ , according to Bao et al. [11]. According to recent research, within four hours following a pig's death, its tissues' conductivity dropped by 10% and its permittivity by 4% [13]. Additionally, it was stated that an animal's aging affected the dielectric characteristics of specific tissues [14]. Wang et al. used the finite-difference time-domain (FDTD) approach to determine the peak of spatial SARs in adult and kid head models exposed to a 900-MHz mobile telephone, and They discovered that there was only a 10% difference in the 1- or 10-g averaged spatial SAR peak with various dielectric characteristics [15]. Keshvari et al. examined how higher dielectric values affected the SAR in brain tissues and discovered that an increase in dielectric value of up to 20% did not equate to an increase in volume-averaged SAR. Consistently resulted in a SAR variation of less than 20% [16]. According to Kang and Gandhi, a 2:1 change in the tissue-simulated liquid's conductivity caused a variation in 1- and 10-g. SAR maximum averages within  $\pm 4\%$  for the 5–6 GHz range and  $\pm 10\%$  for the 2.45 GHz band [17]. Changes in the bodily tissues' dielectric characteristics may have an impact on the input return losses of IWDs. When a pig was put to sleep in a lab, Xu et al. observed that the radiation properties of an IWD inserted in the animal's small intestine changed [18]. The IWD's operation frequency would almost cut in half when it was ingested by the pig,

and the new operation frequency would vary depending on the area. On the other hand, the operation frequency would rise from about 8% to 22% if the pig was put down within a single hour. Electromagnetic modeling for simulation needs to account for these uncertainties and variations. Harun et al. examined the range of permittivity values used in the SAR computation and discovered that, on average, the average SAR was inversely related to permittivity [19]. They also made the observation that it would be necessary to estimate how much SAR results depend on variations in dielectric values. After examining the IWD radiation characteristics' variability at 430 MHz, we discovered that the SAR variation was less than 10% within a 20% range of dielectric values [20]. For video transmission, 434 MHz is the most widely utilized frequency among all commercially available wireless capsule endoscopes [5]. Some publications also use the frequency of 315 and 400–500 MHz [21]. As of late, 2.4 and 1.2 GHz are The purpose of this work is to examine how the dielectric qualities of human body tissues affect the radiation characteristics of IWD inserted into the small intestine at operating frequencies of 800, 1200, and 430 MHz. The analysis of the electromagnetic interaction with the human body is done using the FDTD approach [24]. The structure of this document is as follows. Section II provides a description of the models and techniques used in this work. Variations of SARs and nearby fields are shown in Section III. Section IV offers a final debate and conclusion.

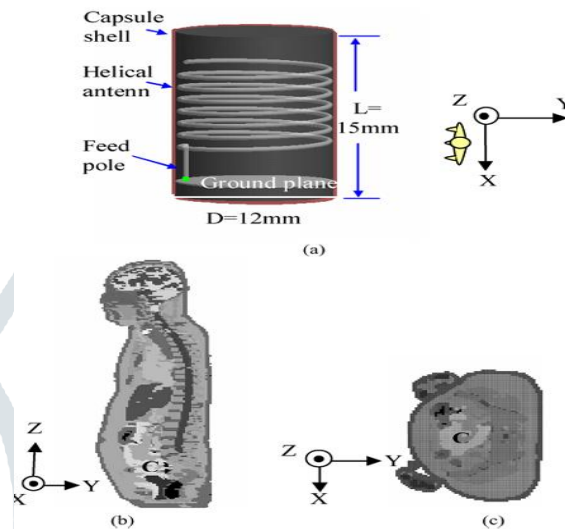


Fig. 1. Simulation configuration. (a) Capsule model of a longitudinal-oriented IWD. (b) Sagittal slice of human model. (c) Transverse slice of human model. C denotes the center of the abdomen area where includes small intestine.

## II. MODELS & METHODS

### A. Models of the Human Body

The Hershey Medical Center's Nuclear Magnetic Resonance (NMR) Group constructed the two human body models used in this work using data on the visible human body, and the electric characteristics of human biological tissues are examined in light of Gabriel et al.'s findings [25]. The height of the high-fidelity female body model is 173 cm. The total number of cells in the female body mesh is  $251 \times 162 \times 642$ , which includes a buffer of 20 free-space cells between the body and the outer edge of the FDTD workspace. The information about permittivity, conductivity, and density related to different frequencies is contained in each cell. There are 23 distinct tissue types in the high-fidelity male body mesh. It is scaled to the same height as the female body model in this instance. Initially, we employ the original tissues in the human body by roughly 10% and 20%, respectively. Next, we adjust all of the human body tissues' relative permittivities by  $\pm 10\%$  and  $\pm 20\%$ , respectively. Lastly, we concurrently alter all of the human body tissues' relative permittivities and conductivities by  $\pm 10\%$  and  $\pm 20\%$ , respectively. For the female and male body models, we thus examine these 39 scenarios with various dielectric values for each operation frequency between 430, 800, and 1200 MHz.

### B. Model of Source

Fig. 1(a) shows the IWD model. The plastic capsule shell has a thickness of 1 mm. The IWD measures 12 mm in diameter and 15 mm in length, respectively. The feed pole measures 2 mm in length and 1 mm in diameter. Air flows through the IWD's interior. In contrast to previous implantable antennas, the ingestible antenna ought to be tiny and omnidirectional. In this case, helical antenna characteristics are tuned for 430, 800, and 1200 MHz of operation. Even while FDTD can simulate the anatomically precise human body structure, tiny antenna modelling remains extremely challenging [24]. Actually, the FDTD system makes use of a variety of techniques [26], [27]. Koulouridius and Nikita examined the accuracy of the FDTD technique's modelling of helix antennas in relation to the findings of the semi analytical approach [Green/method of SAR and the 10-g mean SAR order of 10% [28]. The FDTD grids' approximate rectangular helix is used to build the helical antenna [28]. Because the helical antenna's radius is at most one-fourth of the cell size, the thin single-component helical antenna model is used, much like in [29]. In the GI tract, IWD might move and spin in any direction. The simulations in this case are modeled in Cartesian coordinates, just like in [9], with the Z-axis defined in vertical orientation from foot to head, the Y-axis defined in transversal orientation from anterior to posterior, and the X-axis defined in longitudinal orientation from right to left of the human models. As seen in Fig. 1, the abdomen's center is represented by C.

### C. Method of Computation

The current density, SAR, and power density are the metrics that are most commonly employed to characterize the fundamental features of exposure to an electromagnetic field (EMF). Most people agree that SAR is the best metric to use for assessing the radiation effect of an RF source in close proximity [2], [3]. Here, SAR and near fields are computed using the FDTD approach, which is based on the IEEE's approved numerical computational procedures [30]. The bioheat equation and SAR readings are used to compute the corresponding temperature rise. The maximums of 1- and 10-g averaged SARs are computed and compared with the International Commission on Non-Ionizing Radiation Protection (ICNIRP) and the American National Standards

Institute (ANSI)/IEEE limitations in order to assess the biological effects associated with implantable or ingestible antennas, electric fields, and peak of SAR [2], [3]. The whole-body average SAR mostly determines the body core temperature elevation [31]. Because IWD has less power.

**III. Results**

The IWD sources are positioned in the middle of the human model's GI tract for simulations, as shown in Fig. 1. Since the edible antenna in Figure 1(a) is air-insulated rather than in direct contact with biological tissue, it can prevent high local SAR while also having some potential to enhance communication connection performance[6]. A sagittal slice and a transverse slice of the female body model are shown in Figs. 1(b) and (c). The computed SAR values are displayed as percentage bar graphs, each representing a possible scenario with altered dielectric parameters. For the two human body models, the variations in SARs and electric fields have been estimated for frequencies of 430, 800, and 1200 MHz with longitudinal, transversal, and vertical orientations.

**A. 433 MHz**

It is observed that while the maximums of SAR decrease as conductivities rise, the maximums of SAR sometimes falls as the relative permittivity's rise. Nonetheless, the averaged SAR rises with a relative permit increase and falls with a conductivity increase. Trinities in body models who are male and female. Compared to the male body model, the unaveraged SARs in the female body model are higher, while the averaged SARs are less. The IEEE safety level guidelines stipulate that a wireless device's maximum spatial-average SAR must exceed 1.6 W/kg when averaged across a single 1 g tissue in the form of a cube [2]. The limit is 2 W/kg averaged across any 10 g contiguous tissue, according to ICNIRP safety standards [3]. The highest averaged 1- and 10-g SARs in this case are 3.16 and 0.89 W/kg, respectively. Consequently, these simulation results show that the IWD can be used safely in clinical settings The peak-to-average SAR value in the near-field radiation of IWD is usually greater than the ratio of mobile phone radiations. Consequently, the high-local despite the low input power of IWD, the deposition of radiofrequency radiation in the human body must be carefully taken into account [32]. When human body tissues' conductivities and permittivity's rise to 20%, the greatest variances in SARs, both averaged and averaged, are less than 10%. The maximum of averaged and averaged SAR values will rise in tandem with an increase in conductivities. The maximum of SAR typically falls as relative permittivity rises. Furthermore, 10-g averaged SAR variance is frequently lower than 1-g averaged SAR variation [20]. The strength of the electric

**B. Frequency of 800 MHz**

It is also observed that the dielectric properties of human body tissues have a significant impact on port impedance fluctuations. As conductivity rises, so does the input impedance. In response to an increase in relative permittivity, the real part of the input impedance falls and the imaginary part increases. In most cases, the imaginary part of input impedance will be greater than the sum of the conductivities or relative permittivity's alone when both are increased concurrently. These findings are supported by the body models of both genders. When conductivities rise, SAR maximums rise as well; yet, when relative permittivity's rise, SAR maximums occasionally fall. The As a result, these modelling results show that the IWD can be used in clinics safely with input powers between 9.3 and 62 mW. Based on the safety limits specified by the IEEE and ICNIRP, respectively

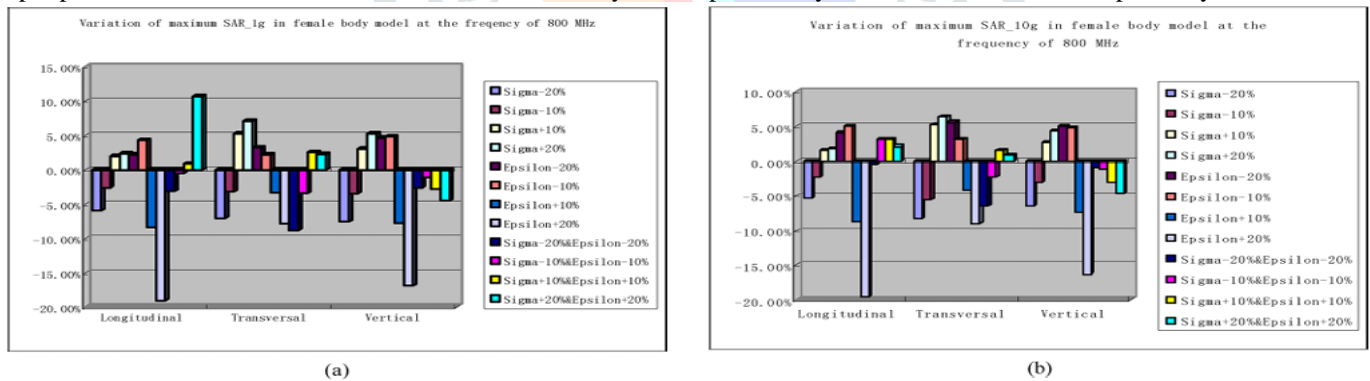


Fig. 2. Variations of maximum of averaged 1- and 10-g SAR in the female body model with different dielectric properties at the operation frequency of 800 MHz. (a) Variation of maximum of averaged 1-g SAR. (b) Variation of maximum of averaged 10-g SAR.

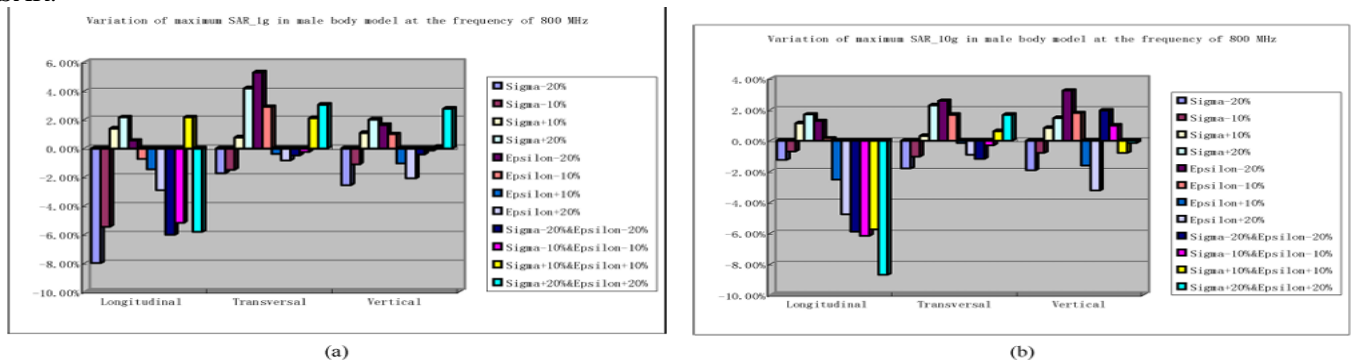


Fig. 3. Variations of maximum of averaged 1- and 10-g SAR in the male body model with different dielectric properties at the operation frequency of 800 MHz. (a) Variation of maximum of averaged 1-g SAR. (b) Variation of maximum of averaged 10-g SAR.

The changes in the maximum SAR values of the male and female body models corresponding to the 800 MHz frequency are shown in Figs. 2 and 3. The fluctuations of the highest amount of When the conductivities and permittivities of human body tissues increase by up to 20%, the unaveraged and averaged SARs are less than 20%. The maximum of averaged and unaveraged SAR values will rise in tandem with an increase in conductivities. The maximum of SAR often falls as the relative permittivity

rises. Furthermore, SAR is far more influenced by relative permittivity than by conductivity. Compared to the female body model, the male body model has a lesser SAR variation. Table I shows the electric fields that FDTD anticipated to be present outside the female body models and close to the abdomen of the human body models. The electric field's intensity was 2.6 dB. changes at the 800-MHz frequency when the dielectric properties shift by 20%. The cases where the conductivities decrease by 20% and by 20%, respectively, correspond to the highest and lowest intensity of the electric field outside the human body model. The variations in electric fields are comparable to those at 430 MHz as well.

**C. 1200 MHz**

It has been noted that the SAR maximums and input impedance fluctuations are comparable to those at the frequency of 800 MHz. The highest averaged 1- and 10-g SAR values in this case are 4.76 and 0.76 W/kg, respectively. According to the IEEE and ICNIRP guidelines for safety levels, these simulation findings thus show that the IWD is safe to be used in clinics with input power less than 8.4 and 64 mW. The changes in the highest SAR values of the male and female body models corresponding to the frequency of 1200 MHz are shown in Figs. 4 and 5. When the permittivities and conductivities of human body tissues change by 20%, the maximum variances of the unaveraged and averaged SARs are less than 30%. The maximum of averaged and unaveraged SAR values will rise as conductivities rise. The maximum of SAR typically increases as the relative permittivity declines. Furthermore, the 10-g averaged SAR frequently varies less than the 1-g averaged SAR. The SAR may rise or fall if both relative permittivity and conductivity rise.

TABLE I  
MINIMUMS AND MAXIMUMS OF THE ELECTRIC FIELDS IN THE AREA WHERE THE RECEIVER IS PLACED ON THE SURFACE OF THE ABDOMEN OF HUMAN BODY MODELS IN DECIBELS AT THE FREQUENCY OF 800 MHZ

Model Orientation	Female body model			Male body model		
	Longitudinal	Transversal	Vertical	Longitudinal	Transversal	Vertical
Original	-9.5 / -15.4 dB	-12.7 / -21.5 dB	-9.4 / -15.0 dB	-5.9 / -12.1 dB	-10.6 / -18.7 dB	-7.1 / -12.9 dB
$\sigma$ -20%	-9.9 / -14.1 dB	-12.6 / -20.9 dB	-8.1 / -13.6 dB	-6.0 / -10.9 dB	-9.7 / -17.5 dB	-6.3 / -12.1 dB
$\sigma$ -10%	-10.2 / -14.7 dB	-13.2 / -21.5 dB	-8.6 / -14.1 dB	-6.1 / -11.7 dB	-10.7 / -18.1 dB	-7.2 / -12.3 dB
$\sigma$ +10%	-11.0 / -15.6 dB	-14.6 / -22.3 dB	-10.0 / -15.5 dB	-6.5 / -12.9 dB	-11.6 / -19.1 dB	-7.9 / -13.2 dB
$\sigma$ +20%	-11.3 / -15.8 dB	-15.1 / -23.4 dB	-10.7 / -16.2 dB	-7.6 / -15.2 dB	-12.8 / -19.9 dB	-8.8 / -14.1 dB
$\epsilon$ -20%	-10.7 / -16.0 dB	-14.6 / -22.5 dB	-10.6 / -16.0 dB	-6.8 / -12.9 dB	-12.7 / -19.7 dB	-9.1 / -14.2 dB
$\epsilon$ -10%	-10.5 / -15.6 dB	-13.7 / -22.0 dB	-10.1 / -15.9 dB	-6.5 / -12.7 dB	-12.4 / -19.8 dB	-8.9 / -13.7 dB
$\epsilon$ +10%	-10.3 / -15.4 dB	-13.2 / -22.5 dB	-8.9 / -14.1 dB	-6.3 / -12.1 dB	-10.2 / -17.7 dB	-7.1 / -12.8 dB
$\epsilon$ +20%	-10.1 / -15.2 dB	-14.3 / -22.8 dB	-9.5 / -13.7 dB	-6.1 / -11.7 dB	-9.8 / -17.6 dB	-6.5 / -12.4 dB
$\sigma$ -20%& $\epsilon$ -20%	-9.9 / -14.7 dB	-13.0 / -21.1 dB	-9.6 / -15.0 dB	-6.4 / -11.8 dB	-12.1 / -19.3 dB	-7.3 / -13.1 dB
$\sigma$ -10%& $\epsilon$ -10%	-10.3 / -15.2 dB	-13.6 / -21.5 dB	-9.5 / -14.7 dB	-6.5 / -12.4 dB	-11.1 / -18.6 dB	-7.2 / -13.0 dB
$\sigma$ +10%& $\epsilon$ +10%	-11.0 / -16.7 dB	-15.1 / -23.3 dB	-9.7 / -14.9 dB	-6.7 / -13.1 dB	-11.2 / -18.7 dB	-8.9 / -14.2 dB
$\sigma$ +20%& $\epsilon$ +20%	-11.1 / -16.3 dB	-14.8 / -23.4 dB	-9.6 / -15.1 dB	-7.2 / -13.6 dB	-10.5 / -18.1 dB	-8.0 / -13.5 dB

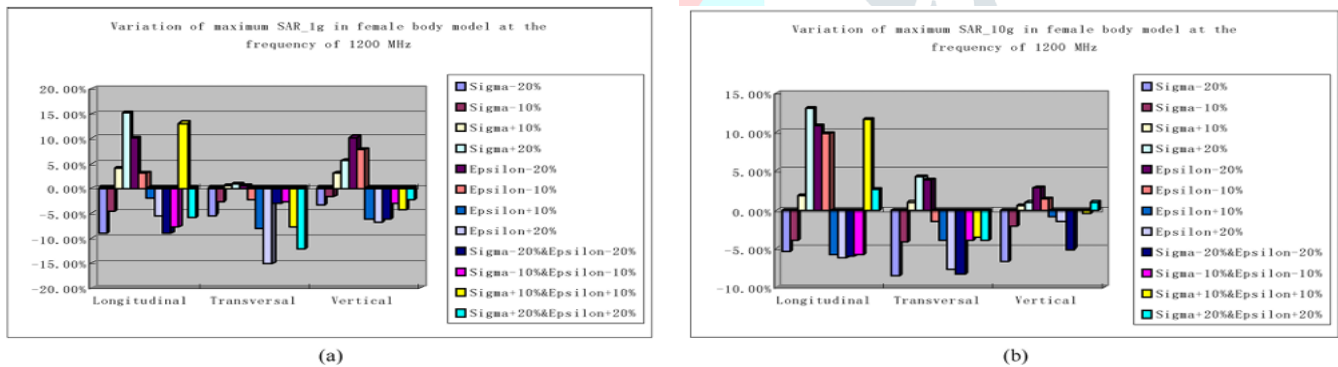


Fig. 4. Variations of maximum of averaged 1- and 10-g SAR in the female body model with different dielectric properties at the operation frequency of 1200 MHz. (a) Variation of maximum of averaged 1-g SAR. (b) Variation of maximum of averaged 10-g SAR.

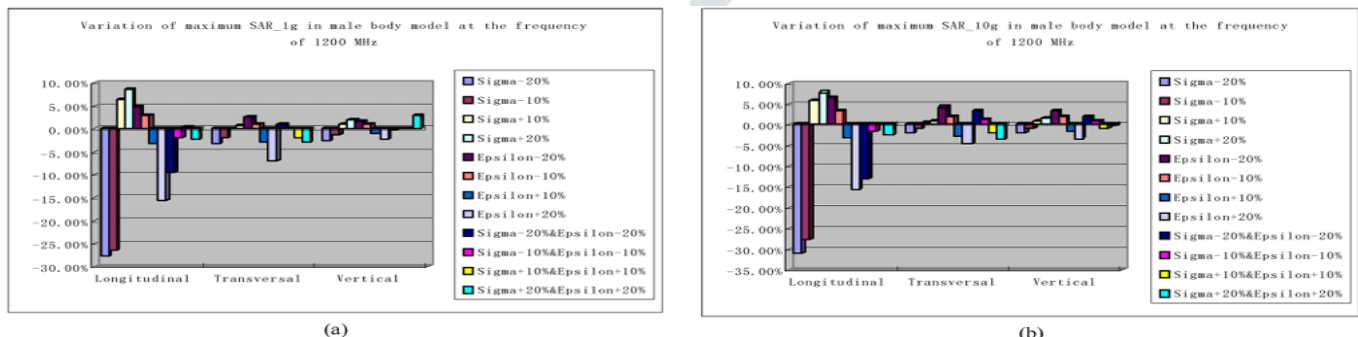


Fig. 5. Variations of maximum of averaged 1- and 10-g SAR in the male body model with different dielectric properties at the operation frequency of 1200 MHz. (a) Variation of maximum of averaged 1-g SAR. (b) Variation of maximum of averaged 10-g SAR

The highest and minimum electric fields outside the female body model and close to the abdomen of the human body models that FDTD predicted are listed in Table II. The electric field's intensity changes by about 3.5 dB when the dielectric parameters shift by 20%. The scenarios where conductivities fall by 20% and rise by 20%, respectively, correspond to the highest and lowest levels of electric field intensity outside the human body model. The electric field maximums within human body models are approximately 40 dB higher than the electric field maximums outside of the models.

TABLE II  
MINIMUMS AND MAXIMUMS OF THE ELECTRIC FIELDS IN THE AREA WHERE THE RECEIVER IS PLACED ON THE SURFACE OF THE ABDOMEN OF HUMAN BODY  
MODELS IN DECIBELS AT THE FREQUENCY OF 1200 MHZ

Model Orientation	Female body model			Male body model		
	Longitudinal	Transversal	Vertical	Longitudinal	Transversal	Vertical
Parameters						
Original	-11.3 / -15.7 dB	-14.3 / -23.1 dB	-10.4 / -15.9 dB	-7.8 / -14.1 dB	-11.6 / -18.9 dB	-8.1 / -14.3 dB
$\sigma$ -20%	-10.9 / -14.8 dB	-13.6 / -21.2 dB	-9.4 / -14.8 dB	-7.0 / -11.9 dB	-11.4 / -19.1 dB	-7.1 / -13.0 dB
$\sigma$ -10%	-11.1 / -15.1 dB	-13.3 / -22.1 dB	-9.6 / -13.2 dB	-7.5 / -12.6 dB	-11.7 / -19.5 dB	-8.2 / -14.8 dB
$\sigma$ +10%	-11.7 / -16.4 dB	-14.9 / -23.3 dB	-12.9 / -16.4 dB	-8.0 / -14.2 dB	-12.6 / -20.5 dB	-9.2 / -14.9 dB
$\sigma$ +20%	-12.0 / -17.3 dB	-16.1 / -24.0 dB	-11.7 / -17.0 dB	-8.6 / -15.2 dB	-13.8 / -21.5 dB	-9.8 / -15.3 dB
$\varepsilon$ -20%	-11.5 / -16.5 dB	-15.6 / -23.9 dB	-11.5 / -16.7 dB	-8.1 / -14.2 dB	-13.7 / -21.1 dB	-10.1 / -15.8 dB
$\varepsilon$ -10%	-11.7 / -16.6 dB	-14.7 / -23.1 dB	-11.0 / -16.5 dB	-7.6 / -13.7 dB	-13.6 / -20.9 dB	-10.0 / -15.1 dB
$\varepsilon$ +10%	-11.4 / -16.1 dB	-14.5 / -23.5 dB	-9.6 / -15.0 dB	-7.3 / -13.3 dB	-11.2 / -18.7 dB	-9.1 / -14.0 dB
$\varepsilon$ +20%	-11.3 / -16.4 dB	-15.3 / -23.6 dB	-9.5 / -14.6 dB	-7.1 / -13.0 dB	-10.3 / -18.4 dB	-7.5 / -13.5 dB
$\sigma$ -20% & $\varepsilon$ -20%	-10.7 / -15.3 dB	-14.8 / -21.4 dB	-10.8 / -16.1 dB	-7.5 / -13.2 dB	-13.8 / -20.6 dB	-8.4 / -14.5 dB
$\sigma$ -10% & $\varepsilon$ -10%	-11.2 / -15.9 dB	-16.6 / -22.3 dB	-10.4 / -15.7 dB	-7.6 / -13.4 dB	-12.5 / -19.7 dB	-8.2 / -14.3 dB
$\sigma$ +10% & $\varepsilon$ +10%	-11.9 / -16.6 dB	-16.1 / -24.1 dB	-10.8 / -16.0 dB	-7.9 / -14.0 dB	-12.1 / -19.8 dB	-9.9 / -15.7 dB
$\sigma$ +20% & $\varepsilon$ +20%	-12.1 / -16.2 dB	-15.6 / -24.7 dB	-10.7 / -16.1 dB	-8.1 / -14.3 dB	-11.5 / -19.7 dB	-9.0 / -14.7 dB

In comparison to the posterior of the human body model, the electric fields in the anterior region are higher. The human body models' left lateral electric fields are comparable to those in the human body model's right lateral. Because the models have distinct structures and shapes, the near field contours when the IWD is placed in the female model differ from those when the IWD is placed in the male model. This is due to the fact that the models of men and women differ in terms of tissue volume and distribution in addition to height and weight [33]. Additionally, Wong and Wiart discovered that the geometry might cause some variation [34].

#### IV. DISCUSSION AND CONCLUSION

The variability of averaged SAR values and nearfield soft the IWD in realistic human body models has been examined in this work. Thirteen scenarios were created by altering the dielectric values by  $\pm 10\%$  and  $\pm 20\%$  at 430, 800, and 1200 MHz, in that order. The findings indicate that there is a 2.5 variance in the electric field intensities close to the human body's midsection. 2.6, and 3.5 dB for the chosen frequencies of 430, 800, and 1200 MHz, respectively, when all dielectric parameters change within a 20% range. Every electromagnetic field at close proximity to the human body's surface is the highest at 20% increase in relative permittivities, and the lowest electric fields at 20% increase in conductivity across all three operating frequencies and two realistic human body models. We may assume that the SAR value would rise as the dielectric values increased based on the SAR calculation equation. With an increase in dielectric values, not even the maximum peak SAR value increases. Unaveraged and averaged SAR measurements are actually impacted by more than only the dielectric characteristics of the Compared to the male body model, the female body model has greater SAR depositions. Raising the dielectric parameters wouldn't guarantee a rise in SAR. In certain cases, the SAR drops. The SAR is reliant on the RF source's operating frequency and orientation. The frequency of 800MHz is where the greatest SAR is found. Less than 10%, 20%, and 30% of the maximum SAR values vary when the dielectric characteristics change by up to 20% at 430, 800, and 1200 MHz, respectively. Regarding the safety level, we must include a factor that takes into account the variation in the dielectric characteristics of biological tissues among different people. These findings imply that an estimate of the relationship between the computed radiation properties of IWD and the Keshvari et al. discovered that as conductivity and permittivity increased throughout the computational field, the maximum peak SAR value in a single voxel increased as well. values [16]. Still, the increase in conductivity is primarily enhanced the local averaged and unaveraged SAR value maximums, whereas the local averaged and unaveraged SAR value maximums are primarily reduced by an increase in permittivity alone. The RF dosimetry calculations utilizing high-fidelity female and male body models validate these findings. Gandhi and Kang discovered that models had little effect at higher frequencies [17]. However, after researching how dielectric values affect the radiation properties of IWD, we discover that some of the findings differ from those of radiation sources external to the human body [18]. There is frequency dependence in the SAR fluctuation. The SAR variation is greater at 1200 MHz operation than it is at 430 and 800 MHz. SAR's fluctuation in relation to dielectric properties is The transceiver design, power consumption, and safety guidelines of in-body radio frequency communication systems need to be carefully taken into consideration. The displayed Analysis yields new and practical knowledge for the design of wireless implants and edible gadgets in the future. This study also shows that, despite the fact that the SARs and electric field distributions of the male and female body models differ at the same dielectric values, the same increment in dielectric values produced essentially the same variances in both SAR and electric field. This publication does not contain all of the work that was done. Future research will be done on a number of other relevant issues, including communication method and RF interference.

#### References

- [1] P. S.Hall andH.Yang, *Antennas and Propagation for Body-Centric Wireless Communications*. London, U.K.: Artech House, 2006.
- [2] IEEE Standard for Safety Levels With Respect to Human Exposure to RadiofrequencyElectromagneticFields,3kHzto300GHz,IEEEStandard C95.1, 1999.
- [3] International Commission on Non-Ionizing Radiation Protection, "Guide lines for limiting exposure to time-varying electric, magnetic, and elec tromagnetic fields (up to 300 GHz)," *Health Phys.*, vol. 74, pp. 494–522, 1998.
- [4] H. Virtanen, J. Keshvari, and R. Lappalainen, "The effect of authentic metallicimplantsontheSARdistributionoftheheadexposedto900,1800, and 2450 MHz dipole near field," *Phys. Med. Biol.*, vol. 52, pp. 1221–1236, 2007.
- [5] G.D.Meron, "The development of the swallowable videocapsule (M2A)," *Gastrointest. Endosc.*, vol. 52, pp. 817–819, Dec. 2000.
- [6] R. S. Yahya and J. H. Kim, "Implanted antennas in medical wire less communications," *Synth. Lect. Antennas*, vol. 1, no. 1, pp. 1–82, 2006.
- [7] E. A. Johannessen, L. Wang, L. Cui, T. B. Tang, M. Ahmadian, A. Astaras, S. W. J. Reid, P. S. Yam, A. F. Murray, B. W. Flynn, S. P. Beaumont, D. R. S. Cumming, and J. M. Cooper, "Implementation of multichannel sensors for remote biomedical measurements in a microsys temsformat," *IEEETrans.Biomed.Eng.*, vol.51,no.3,pp.525–535,Mar. 2004.
- [8] J. E. Pandolfino, J. E. Richter, T. Ours, J. M. Guardino, J. Chapman, and P. J. Kahrilas, "Ambulatory esophageal pH monitoring using a wireless system," *Amer. J. Gastroenterol.*, vol. 98, no. 4, pp. 740–749, 2003.

- [9] L. C. Chirwa, P. A. Hammond, S. Roy, and D. R. S. Cumming, "Electro magnetic radiation from ingested sources in the human intestine between 150 MHz and 1.2 GHz," *IEEE Trans. Biomed. Eng.*, vol. 50, no. 4, pp. 484–492, Apr. 2003.
- [10] L. S. Xu, M. Q.-H. Meng, H. L. Ren, and Y. W. Chan, "Radiation characteristics of ingestible wireless devices in human intestine following radio frequency exposure at 430, 800, 1200 and 2400 MHz," *IEEE Trans. Antennas Propag.*, vol. 57, no. 8, pp. 2418–2428, Aug. 2009.
- [11] J. Z. Bao, S. T. Lu, and W. D. Hurt, "Complex dielectric measurements and analysis of brain tissues in the radio and microwave frequencies," *IEEE Trans. Microw. Theory Tech.*, vol. 45, no. 10, pp. 1730–1741, Oct. 1997.
- [12] C. Gabriel and A. Peyman, "Dielectric measurement: Error analysis and assessment of uncertainty," *Phys. Med. Biol.*, vol. 51, pp. 6033–6046, 2006.
- [13] G. Schmid, G. Neubauner, M. I. Udo, and A. Francois, "Dielectric properties of porcine brain tissue in the transition from life to death at frequencies from 800 to 1900 MHz," *Bioelectromagnetics*, vol. 24, pp. 413–422, 2003.
- [14] A. Peyman, S. J. Holden, S. Watts, R. Perrott, and C. Gabriel, "Dielectric properties of porcine cerebrospinal tissues at microwave frequencies: In vivo, in vitro and systematic variation with age," *Phys. Med. Biol.*, vol. 52, pp. 2229–2245, 2007.
- [15] J. Q. Wang, O. Fujiwara, and S. Watanabe, "Approximation of aging effect on dielectric tissue properties for SAR assessment of mobile telephones," *IEEE Trans. Electromagn. Compat.*, vol. 48, no. 2, pp. 408–413, May 2006.
- [16] J. Keshvari, R. Keshvari, and S. Lang, "The effect of increase in dielectric values on specific absorption rate in eye and head tissues following 900, 1800, and 2450 MHz radio frequency exposure," *Phys. Med. Biol.*, vol. 51, pp. 1463–1477, 2006.
- [17] G. Kang and O. P. Gandhi, "Effect of dielectric properties on the peak 1 and 10-g SAR for 802.11 a/b/g frequencies 2.45 and 5.15 to 5.85 GHz," *IEEE Trans. Electromagn. Compat.*, vol. 46, no. 2, pp. 268–274, May 2004. [18] L. S. Xu, M. Q. H. Meng, Y. W. Chan, C. Hu, and H. B. Wang, "Influence of anesthetic and dead animal bodies on ingested wireless device," in *Proc. IEEE/ASME Int. Conf. Adv. Intell. Mechatronics*, Xi'an, China, Jul. 2–5, 2008, pp. 176–180.
- [19] W. D. Hurt et al., "Variability in EMF permittivity values: Implications for SAR calculations," *IEEE Trans. Biomed. Eng.*, vol. 47, no. 3, pp. 396–401, Mar. 2000.
- [20] L. S. Xu, M. Q.-H. Meng, and Y. W. Chan, "Effects of dielectric parameters of human body on radiation characteristics of ingestible wireless device at operating frequency of 430 MHz," *IEEE Trans. Biomed. Eng.*, vol. 56, no. 8, pp. 2083–2094, Aug. 2009.
- [21] H. J. Park, H. W. Nam, B. S. Song, J. L. Choi, H. C. Choi, J. C. Park, M. N. Kim, J. T. Lee, and J. H. Cho, "Design of bi-directional and multi channel miniaturized telemetry module for wireless endoscopy," in *Proc. 2nd Annu. Int. IEEE-EMBS Spec. Topic Conf. Microtechnol. Med. Biol.*, Madison, WI, May 2–4, 2002, pp. 273–276.
- [22] Y. Kim, G. Lee, S. Park, B. Kim, J. O. Park, and J. H. Cho, "Pressure monitoring system in gastro-intestinal tract," in *Proc. 2005 IEEE Int. Conf. Robot. Autom.*, Barcelona, Spain, Apr. 2005, pp. 1321–1326.
- [23] S. G. Han, B. Y. Chi, and Z. H. Wang, "A 2.4 GHz low power ASK transmitter for wireless capsule endoscope applications," *Chin. J. Semicond.*, vol. 27, no. 6, pp. 988–993, 2006.
- [24] A. Taflove and S. C. Hagness, *Computational Electrodynamics: The Finite-Difference Time-Domain Method*, 3rd ed. Norwood, MA: Artech House, 2000.
- [25] S. Gabriel, R. W. Lau, and C. Gabriel, "The dielectric properties of biological tissues: III. Parametric models for the dielectric spectrum of tissues," *Phys. Med. Biol.*, vol. 41, pp. 2271–2293, 1996.
- [26] S. Watanabe and M. Taki, "An improved FDTD model for the feeding gap of a thin-wire antenna," *IEEE Microw. Guided Wave Lett.*, vol. 8, no. 4, pp. 152–154, Apr. 1998.
- [27] P. Bernardi, M. Cavagnaro, S. Pisa, and E. Piuzzi, "A graded-mesh FDTD code for the study of human exposure to cellular phones equipped with helical antennas," *Appl. Comput. Electromagn. Soc. J.*, vol. 16, no. 3, pp. 90–96, 2001. [28] S. Koulouridius and K. S. Nikita, "Study of the coupling between human head and cellular phone helical antennas," *IEEE Trans. Electromagn. Compat.*, vol. 46, no. 1, pp. 62–70, Feb. 2004.
- [29] G. Waldschmidt and A. Taflove, "The determination of the effective radius of a filamentary source in the FDTD mesh," *IEEE Microw. Guided Wave Lett.*, vol. 10, no. 6, pp. 217–219, Jun. 2000.
- [30] IEEE Recommended Practice for Measurements and Computations of Radio Frequency Electromagnetic Fields With Respect to Human Exposure to Such Fields, 100 kHz–300 GHz, IEEE Standard C95.3-2002, 2002.
- [31] A. Hirata, T. Asano, and O. Fujiwara, "FDTD analysis of human body core temperature elevation due to RF far-field energy prescribed in the ICNIRP guidelines," *Phys. Med. Biol.*, vol. 52, pp. 5013–5023, 2007.
- [32] E. R. Adair and R. C. Petersen, "Biological effects of radio frequency/microwave radiation," *IEEE Trans. Microw. Theory Tech.*, vol. 50, no. 3, pp. 953–962, Mar. 2002.
- [33] M. Zankl, K. F. Eckerman, and W. E. Bolch, "Voxel-based models representing the male and female ICRP reference adult—the skeleton," *Radiat. Prot. Dosim.*, vol. 127, pp. 174–186, 2007.
- [34] M. F. Wong and J. Wiart, "Modeling of electromagnetic wave interactions with the human body," *C. R. Phys.*, vol. 6, no. 6, pp. 585–594, 2005. [35] H. Y. Chen and H. P. Yang, "SAR affected by shapes and electrical properties of the human head exposed to a cellular phone," *Microw. Opt. Technol. Lett.*, vol. 42, no. 1, pp. 1–4, 2004.